Supplementary Information for Influence of the Frequency on Undulatory Swimming Speed in Granular Media

Iñaki Echeverría-Huarte, Margarida M. Telo da Gama, and Nuno A. M. Araújo
Centro de Física Teórica e Computacional, Faculdade de Ciências, Universidade de Lisboa, 1749-016 Lisboa, Portugal.
(Dated: July 3, 2024)

In the supplementary information (SI) we provide the theoretical basis for the computation of the normal and resonance modes of the swimmer. We also expand on the technical details regarding the coarse-graining formulation and contact network characterization. Finally, we provide some complementary plots.

Appendix A: Normal and resonance modes of the swimmer

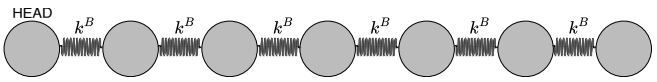

Fig. S1. Representation of the linear chain of coupled oscillators.

To find the resonance modes of the swimmer, we use the undamped model to calculate the natural modes and then adjust the frequencies considering the damping ratio [1]. Thus, we can conceptualize the swimmer as a set of seven masses connected by six springs (Fig. S1). The masses m are all equal except for the mass of the head, which is $m_h = 7\,m$. The spring constants $k \equiv k^B$ are all equal. Let $\vec{x} = (x_1, x_2, \cdots, x_7)$ be the displacements of the masses from the equilibrium position. The equations of motion for x_i are:

$$\begin{aligned} m_h\,\ddot{x}_1 &= -k(x1 - x2) \\ m\,\ddot{x}_2 &= -k(x2 - x1) - k(x2 - x3) \\ m\,\ddot{x}_3 &= -k(x3 - x2) - k(x3 - x4) \\ &\vdots \\ m\,\ddot{x}_7 &= -k(x7 - x6) \end{aligned} \tag{1}$$

This system can be written in matrix form as:

$$\begin{pmatrix} m_h & 0 & 0 & \cdots & 0 \\ 0 & m & 0 & \cdots & 0 \\ 0 & 0 & m & \dots & 0 \\ \vdots & \vdots & \vdots & \ddots & \vdots \\ 0 & 0 & 0 & \cdots & m \end{pmatrix} \frac{d^2}{dt^2} \begin{pmatrix} x_1 \\ x_2 \\ \vdots \\ \vdots \\ x_7 \end{pmatrix} + \begin{pmatrix} k & -k & 0 & \cdots & 0 \\ -k & 2k & -k & \cdots & 0 \\ 0 & -k & 2k & \cdots & 0 \\ \vdots & 0 & 0 & \ddots & -k \\ 0 & 0 & 0 & -k & k \end{pmatrix} \begin{pmatrix} x_1 \\ x_2 \\ \vdots \\ \vdots \\ x_7 \end{pmatrix} = \begin{pmatrix} 0 \\ 0 \\ \vdots \\ \vdots \\ 0 \end{pmatrix} \tag{2}$$

or, more generally,

$$M\frac{d^2\vec{x}}{dt^2} + K\vec{x} = 0 \tag{3}$$

where M and K are the mass and stiffness matrices, respectively. Since we are interested in finding harmonic solutions for $\vec{x}$, we can assume that the solution has the form $\vec{x} = \vec{X}\,sin(\omega t)$, and substitute it into Eq. (3):

$$-M\vec{X}\omega^2 sin(\omega t) + K\vec{X}sin(\omega t) = 0 \rightarrow \tag{4a}$$

$$\rightarrow K\vec{X} = \omega^2 M\vec{X} \tag{4b}$$

The scalar values λ^n that satisfy a matrix equation $K\vec{u} = \lambda M\vec{u}$ are commonly known as the *generalized eigenvalues* of the equation, and are directly associated with the natural frequencies through $\omega_0^n = \sqrt{\lambda^n}$. We have used MATLAB to solve the system for different values of k^B. The frequencies of the first and second normal modes, ω_0^n, and the corresponding resonance modes, ω_r^n, are listed in Table I. Note that to obtain the ordinary frequencies f, we must divide ω by 2π.

Appendix B: Coarse-graining calculation

We obtain macroscopic continuum fields by applying an integrable coarse-graining function $\varphi(\vec{r}, t)$. Specifically, we have opted for a truncated two-dimensional (2D) Gaussian function $\varphi[\vec{r} - \vec{r}_i(t)] = A_\omega^{-1}\exp\left[-(r - r_i)^2/2\omega^2\right]$, where ω, the Gaussian rms

k^B	ξ	Mode **n**	w_0^n	$w_r^n = w_0^n\sqrt{1-2\xi^2}$
100	0.29	1	26.37	23.96
		2	62.59	56.91
150	0.24	1	32.30	30.38
		2	76.66	72.09
200	0.20	1	37.30	35.65
		2	88.52	84.60
500	0.13	1	58.98	57.95
		2	139.96	137.51

TABLE I. The first and second normal modes (ω_0^n) as well as the corresponding resonance modes (ω_r^n) of the swimmer. Different values of k^B have been used. The damping ratio (ξ) corresponding to each k^B is provided in the second column. In all cases, the condition of significantly underdamping ($\xi < 1/\sqrt{2}$) is fulfilled, and the resonance frequency is well defined.

width, has been selected to be equal to the the mean grain radius $\langle r_G \rangle$ of the bulk. This choice strikes a balance between being too small (which would not smooth out as desired) and being too large (which would require significant corrections [2]). Here, A_ω^{-1} is the normalization constant ensuring that φ is normalized in the interval $[-r_c, r_c]$, with $r_c = 3\omega$ the cut-off length. Consequently, the 2D solid fraction field Φ of the system is given at time t as:

$$\Phi(\vec{r},t) = A_P \sum_{i=1}^{N} \varphi[\vec{r} - \vec{r}_i(t)] \tag{5}$$

where $\vec{r}_i$ is the position of each single grain of the granular bed and A_p is the area of the grain. The velocity field $\vec{V}$ is calculated in a similar way:

$$\vec{V}(\vec{r},t) = A_P \sum_{i=1}^{N} \vec{v}_i\, \varphi[\vec{r} - \vec{r}_i(t)]/\Phi(\vec{r},t) \tag{6}$$

where $\vec{v}_i$ is the instantaneous velocity of particle i.

Following the approach outlined in [3, 4], we introduce the macroscopic stress field σ, which can be decomposed into a kinetic stress field (σ^K) and a contact stress field (σ^C). The kinetic stress σ^K takes into consideration the velocity fluctuations with respect to the mean velocity field $\vec{V}(\vec{r},t)$. These fluctuations are expressed as $\vec{v}_i^*(\vec{r},t) = \vec{v}_i(\vec{r},t) - \vec{V}(\vec{r},t)$. The kinetic stress tensor is thus defined as:

$$\sigma^K(\vec{r},t) = \sum_{i=1}^{N} \vec{v}_i^* \otimes \vec{v}_i^*\, \varphi[\vec{r} - \vec{r}_i(t)]. \tag{7}$$

where $\otimes$ is the dyadic product. It is generally accepted that the trace of the kinetic stress, the so called kinetic pressure $p^K(\vec{r},t)$, is proportional to the granular temperature [5, 6]. Defined as $p^K(\vec{r},t) = \mathrm{Tr}(\sigma^K(\vec{r},t))$, it represents a measurement of the grain fluctuations respect to the mean velocity field.

The contact stress tensor σ^C is calculated using the interaction forces $\vec{F}_{ij}$ and branch vectors $\vec{r}_{ij}$ through the line integral of $\varphi(\vec{r},t)$ along $\vec{r}_{ij}$, as follows:

$$\sigma^C(\vec{r},t) = \sum_{i=1}^{N}\sum_{j=1}^{N_c} \vec{r}_{ij} \otimes \vec{F}_{ij} \int_0^1 \varphi[\vec{r} - \vec{r}_i(t) + s\vec{r}_{ij}]\, ds \tag{8}$$

Note that this process applies individually to every single contact N_c of a particle i. As for the kinetic stress case, we can also define the contact pressure $p^C(\vec{r},t)$ as $p^C(\vec{r},t) = \mathrm{Tr}(\sigma^C(\vec{r},t))$ [5]. Finally, the total pressure P is determined by:

$$P(\vec{r},t) = \frac{p^K(\vec{r},t) + p^C(\vec{r},t)}{2} \tag{9}$$

Under stationary conditions, it is possible to characterize all these quantities by computing their mean fields. These mean fields are obtained by averaging the fields over multiple time steps in each simulation, denoted by $\Phi(\vec{r}) = \langle\Phi(\vec{r},t)\rangle$, $\vec{V}(\vec{r}) = \langle\vec{V}(\vec{r},t)\rangle$, $\sigma^K(\vec{r}) = \langle\sigma^K(\vec{r},t)\rangle$, and $\sigma^C(\vec{r}) = \langle\sigma^C(\vec{r},t)\rangle$.

Appendix C: Contact Network

The fabric tensor characterizes the contact network by analyzing the branch vectors $\vec{r}_{ij}$ [7]. For systems with disk-like particles, branch vectors are defined for particle pairs in contact (i.e. when $|\vec{r}_{ij}| \leq R_{ij}$, with r_{ij} denoting the inter-particle distance and R_{ij} representing the sum of their radii). The fabric tensor R is then defined as:

$$R = \sum_{i,j}^{N_c} \vec{r}_{ij} \otimes \vec{r}_{ij} \tag{10}$$

where the summation takes into account all contacts N_c between pairs of particles (i,j). The eigenvalues R_1 and R_2 of this tensor allow us to calculate the average number of contacts per particle $Z = R_1 + R_2$, and the anisotropy of the contact network defined as $\rho = (R_1 - R_2)/Z$.

Appendix D: Extended Figures

Determination of μ_{eff}

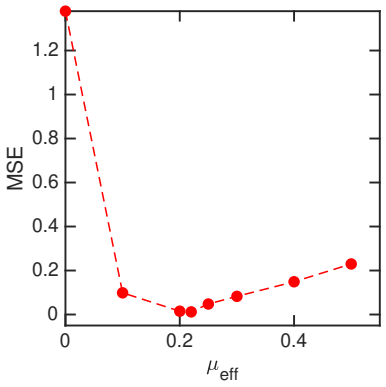

Fig. S2. Mean squared error (MSE) calculated for the curves obtained in Fig. 3a (main text). The curve has a minimum at $\mu_{\text{eff}} = 0.22$, the value used to validate the model in Fig. 3b (main text).

Appendix E: Supplementary Movies

- Movie S1: Simulation in the frictionless granular medium (i.e. $\vec{F}_i^F = 0$) at an oscillation frequency $f = 4Hz$.
- Movie S2: Simulation in the frictionless granular medium (i.e. $\vec{F}_i^F = 0$) at an oscillation frequency $f = 9Hz$.
- Movie S3: Simulation in the frictionless granular medium (i.e. $\vec{F}_i^F = 0$) at an oscillation frequency $f = 15Hz$.

System-size and grain-size effect

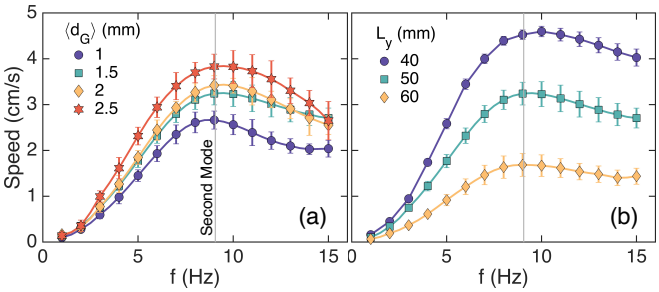

Fig. S3. Swimming speed dependence on frequency for the frictionless system (i.e., $\vec{F}_i^{\text{F}} = 0$) changing (a) average grain size $\langle d_G \rangle$ and (b) system size L_y as indicated in the legend. The vertical solid lines represent the second resonance mode. The system investigated in the main text corresponds to $\langle d_G \rangle = 1.5$ mm and $L_y = 50$ mm. The error bars have been calculated based on the standard error with a confidence level of 95%.

Swimmer size effect

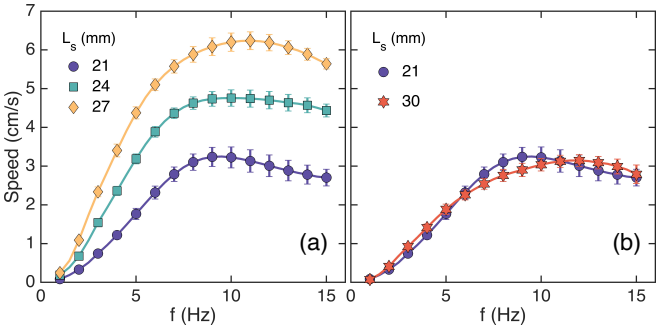

Fig. S4. Swimming speed dependence on frequency for the frictionless system (i.e., $\vec{F}_i^{\text{F}} = 0$). In (a), the length of the swimmer L_s is changed while keeping constant $L_x = 100\,\text{mm}$ and $L_y = 50\,\text{mm}$. In (b), both L_x and L_y are scaled to keep the same ratio between the swimmer length and system size.

[1] D. Morin, *Harvard University*, 2002.
[2] R. Artoni and P. Richard, *Physical Review E*, 2015, **91**, 032202.
[3] M. Babic, *International Journal of Engineering Science*, 1997, **35**, 523–548.
[4] I. Goldhirsch, *Granular Matter*, 2010, **12**, 239–252.
[5] J. H. Irving and J. G. Kirkwood, *The Journal of Chemical Physics*, 1950, **18**, 817–829.
[6] S. M. Rubio-Largo, A. Janda, D. Maza, I. Zuriguel and R. C. Hidalgo, *Physical Review Letters*, 2015, **114**, 238002.
[7] S. C. Cowin, *Mechanics of Materials*, 1985, **4**, 137–147.